Received: 23 December 2023 | Revised: 15 January 2024 | Accepted: 12 February 2024

DOI: 10.1111/iwj.14815

ORIGINAL ARTICLE

IWJ WILEY

HMOX1 as a therapeutic target associated with diabetic foot ulcers based on single-cell analysis and machine learning

Yiqi Chen[1] | **Yixin Zhang**[1,2] | **Ming Jiang**[1] | **Hong Ma**[1,3] | **Yuhui Cai**[1]

[1]Department of Burn and Plastic Surgery, Affiliated Hospital of Nantong University, Nantong, China

[2]Department of Breast Surgery, Yantai City Yantai Hill hospital, Yantai, China

[3]Department of Burn, Hanzhong Central Hospital, HanZhong, China

Correspondence
Yuhui Cai, Department of Burn and Plastic Surgery, Affiliated Hospital of Nantong University, Nantong, Jiangsu Province, China.
Email: cyh-nt@163.com

Funding information
The Nantong Municipal Health Commission General Project Fund, Grant/Award Number: MB2021006

Abstract

Diabetic foot ulcers (DFUs) are a serious chronic complication of diabetes mellitus and a leading cause of disability and death in diabetic patients. However, current treatments remain unsatisfactory. Although macrophages are associated with DFU, their exact role in this disease remains uncertain. This study sought to detect macrophage-related genes in DFU and identify possible therapeutic targets. Single-cell datasets (GSE223964) and RNA-seq datasets (GSM68183, GSE80178, GSE134431 and GSE147890) associated with DFU were retrieved from the gene expression omnibus (GEO) database for this study. Analysis of the provided single-cell data revealed the distribution of macrophage subpopulations in the DFU. Four independent RNA-seq datasets were merged into a single DFU cohort and further analysed using bioinformatics. This included differential expression (DEG) analysis, multiple machine learning algorithms to identify biomarkers and enrichment analysis. Finally, key results were validated using reverse transcription-quantitative polymerase chain reaction (RT-qPCR) and Western bolt. Finally, the findings were validated using RT-qPCR and western blot. We obtained 802 macrophage-related genes in single-cell analysis. Differential expression analysis yielded 743 DEGs. Thirty-seven macrophage-associated DEGs were identified by cross-analysis of marker genes with macrophage-associated DEGs. Thirty-seven intersections were screened and cross-analysed using four machine learning algorithms. Finally, HMOX1 was identified as a potentially valuable biomarker. HMOX1 was significantly associated with biological pathways such as the insulin signalling pathway. The results showed that HMOX1 was significantly overexpressed in DFU samples. In conclusion, the analytical results of this study identified HMOX1 as a potentially valuable biomarker associated with

Yiqi Chen and Yixin Zhang contributes equally to this work.

macrophages in DFU. The results of our analysis improve our understanding of the mechanism of macrophage action in this disease and may be useful in developing targeted therapies for DFU.

KEYWORDS

diabetes foot ulcers, HMOX1, machine learning, single cell analysis

Key Messages

- This study revealed the distribution of macrophage subpopulations as well as the functional status in DFU by single-cell analysis.
- This study identified HMOX1 as a clinically valuable biomarker associated with DFU by four machine learning algorithms (Boruta, XGBoost, SVM and Random forest).
- The analytical results of this study improve our understanding of the mechanism of macrophage action in this disease and may contribute to the development of targeted therapies for DFU.

1 | INTRODUCTION

Diabetes has progressively emerged as a significant global public health issuse.[1] Correspondingly, the global number of diabetes patients was projected to reach 536.6 million by the end of the year 2021. With a constant increase in the number of diabetic patients annually, the global prevalence of diabetes is expected to reach 693 million individuals by the year 2045.[2] Moreover, diabetes is frequently associated with a variety of complications, including peripheral neuropathy, chronic renal failure, cardiovascular disease and diabetic skin wounds or ulcers.[3] In this context, diabetic foot ulcers (DFUs) are considered one of the most serious complications of diabetes. DFU is a condition that occurs in patients with diabetes resulting from nerve abnormalities at the distal end of the lower limbs and varying degrees of vascular disease, involving foot infection, ulcer, and/or deep tissue destruction.[4,5] Possible aetiologies of DFU include smoking, hypertension, hyperglycaemia, diabetic progression, vascular occlusion and neuropathy.[6] As evident from earlier studies, about 537 million individuals worldwide are affected by diabetes, of which 19%–34% of diabetes patients suffer from DFU. Moreover, around 20% of DFU patients require amputation of the lower limb, while 10% of patients experience mortality within 1 year following their initial DFU diagnosis.[7–9] Amputation severely reduces the quality of life for individuals with diabetes, while also resulting in elevated mortality rates and substantial medical expenses.[10] Thus, given their prevalence and capacity to result in disability and death, DFUs represent a critical public health issue that imposes a substantial burden on social and economic well-being. At present, the primary methods of treatment for DFU involve the debridement of wounds, relieving pressure on the wound, controlling blood sugar levels and preventing infection. Several emerging treatment modalities, such as negative pressure wound treatments, dressing changes and hyperbaric oxygen therapy, are progressively being incorporated into clinical practice. However, the therapeutic efficacy of these approaches remains unsatisfactory.[11,12] Hence, it is imperative to further investigate the aetiology of DFU in order to devise novel therapeutic approaches that can aid diabetic patients in both preventing and managing DFU.

Macrophages exhibit diverse phenotypes that are implicated in a range of physiological processes and disease mechanisms.[13] Their capacity to rapidly transform phenotypes plays a crucial role in regulating various aspects of tissue repair.[13] Macrophages are primarily classified into two main types: the pro-inflammatory M1 type and the anti-inflammatory M2 type.[14] The M1 subtype of macrophages appears during the initial tissue damage response, which is triggered by endogenous damage-related molecular patterns or exogenous pathogen-related molecular patterns. They demonstrate heightened phagocytosis and synthesis of pro-inflammatory cytokines, which are essential for innate immunity and wound cleaning. M2 macrophages play a crucial role in the subsequent healing process, as they are activated by various stimuli, aiding in the reduction of inflammation and facilitating the formation and reconstruction of tissues.[15] Both M1 and M2 macrophages are necessary for the progression of wound healing; correspondingly, macrophages have been implicated in wound healing processes, including DFU.[14,16,17] A recent study conducted by Aitcheson et al., demonstrated that hyperglycaemia, can lead to an increase in the ratio of M1 macrophages in

comparison to M2 macrophages.[18] Thus, modulating the equilibrium between M1 and M2 macrophages could offer a promising approach for treating DFUs. In this context, macrophages may have the potential to function as effective therapeutic targets for DFU.[19] However, the specific mechanism by which macrophages operate in the context of DFU remains unidentified.

The advancement of genomics and bioinformatics research technology has facilitated the development and enhancement of disease databases, which serve as a theoretical foundation for the identification of novel therapeutic targets and disease mechanisms. In recent years, the field of bioinformatics has been extensively utilized to investigate targets for tumours and other diseases.[20–23] At the same time, the high accuracy and specificity of single-cell sequencing technologies have rendered them an ideal tool for single-cell research. The use of single-cell sequencing technology facilitates high-throughput, unbiased analysis of even extremely small sample sizes. This allows for the identification of cell specificity and variations within cells from a localization-based perspective, facilitating the investigation of cooperative interactions between cells and the examination of tissue heterogeneity. Moreover, single-cell sequencing technologies enable researchers to gain a more comprehensive understanding of the dynamic alterations occurring in genes and proteins.[24–26] As a result, the present study employs single-cell data analysis and RNA sequencing data to investigate the mechanism of macrophage action in DFU, offering a theoretical and experimental framework for the treatment of DFU.

2 | METHODS

2.1 | Download and processing of DFU-related datasets

The workflow of our study is shown in Figure 1. We obtained the DFU-associated single-cell dataset (GSE223964) from the GEO database. At the same time, we acquired four independent DFU-related RNA seq datasets from the GEO database. These included the GSE68183, GSE80178, GSE134431 and GSE147890 datasets. The GSE68183 dataset comprised of three samples from patients with DFU and three samples from individuals without DFU, serving as normal controls. On the other hand, the GSE80178 dataset contained nine disease samples and three normal samples. Conversely, the GSE134431 dataset contained 21 disease samples, while the GSE147890 dataset contained 12 disease samples and 12 normal samples. In addition, the 'Combat' algorithm, available in the R package 'SVA', was employed to mitigate batch effects across multiple datasets and integrate four distinct RNA seq datasets into a single unified dataset.

2.2 | Single-cell analysis

The Seurat package was utilized for cell clustering, employing t-distribution random neighbour embedding (t-SNE) analysis and principal component analysis (PCA). By filtering out cells with mitochondrial genes <200, >2500 or >5%, data filtering was performed to ensure the quality of the analysis results. Subsequently, after data normalization, 2000 highly variable genes were identified using the 'VST' approach. Following that, PCA was performed to identify significant principal components (PCs). Finally, a total of 25 PCs were selected for the t-SNE analysis. The FindClusters function was then used to categorize cells into 10 separate clusters, with a resolution of 1.5.

2.3 | Identification and functional annotation of differential expression analysis

Within the DFU queue, we employed the 'limma' package to identify DEGs, utilizing thresholds of $|\log2FC| > 1$ and $p < 0.05$. The R packages 'Pheatmap' and 'ggplot2' were utilized to create thermal and volcanic maps of DEGs. Subsequently, we compared DEGs with specific genes that served as markers for different subpopulations of macrophages in a single-cell dataset. Following that, functional annotation was conducted on the acquired cross genes. Subsequently, the R package 'clusterProfiler' was used to conduct gene ontology (GO) and Kyoto Encyclopedia of Genes and Genomes (KEGG) pathway enrichment analysis to identify the significant pathways having a p-value threshold of <0.05.

2.4 | Identification of potential biomarkers for DFU based on four machine algorithms

We utilized four machine-learning algorithms to analyse the intersection genes obtained previously, aiming to identify potential biomarkers associated with DFU. These included commonly used feature selection algorithms such as random forest algorithm (RF), XGBoost, support vector machine recursive feature elimination (SVM-RFE) and Boruta feature selection model, which were then used to filter the feature basis of DFUs. Extreme gradient

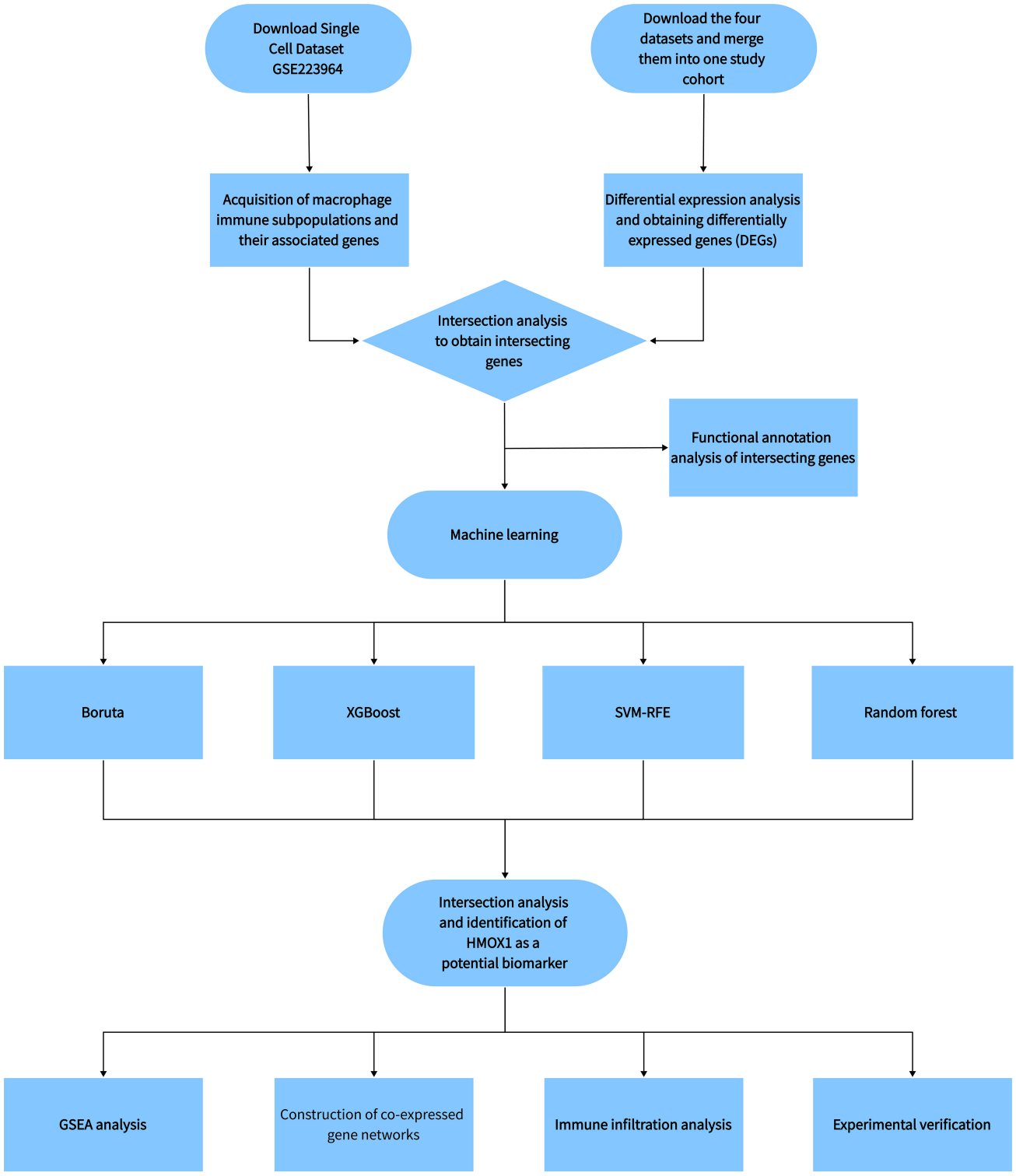

FIGURE 1 The flow chart of our study.

boosting (XGBoost) is a widely employed algorithm for supervised integrated learning. The algorithm utilizes a gradient-enhanced tree model to effectively address classification and regression problems. XGBoost also has the capability to utilize the expression values of important genes as feature values for training the model. By providing the expression values of key genes as feature values to the XGBoost model, these features can be used for classification or regression tasks.[27] On the other hand, RF comprises a type of supervised machine learning

approach that employs random forest algorithms to categorize or arrange features.[28] Subsequently, to assess the predictive performance and identify characteristic genes, we employed tenfold cross-validation and consider genes with a relative importance >1.5. Additionally, SVM-RFE comprises a widely used machine learning algorithm that simplifies typical classification and regression problems through efficient 'transduction inference' from training to predicting samples.[29] Accordingly, SVM-RFE has been used for screening feature genes through iterative ranking of features in order to mitigate overfitting. On the other hand, the Boruta feature selection method comprises a feature-filtering machine learning method that is primarily based on random forests.[30] By calculating the significance score of each feature and contrasting it with randomly generated shadow features, it can aid in identifying the most pertinent feature genes associated with DFU. All these machine-learning methods can be utilized for the purpose of feature gene selection. Correspondingly, we utilized these algorithms to identify the most pertinent feature genes associated with DFU. Subsequently, we investigated their involvement in disease progression and therapeutic approaches.

In addition to the above, we evaluated the diagnostic accuracy of the biomarkers and analysed the gene expression in the DFU cohort. The biomarker expression levels in samples from patients with DFU and samples from healthy individuals were compared using the independent *t*-test, and the significance level was set at $p < 0.05$. The diagnostic utility of biomarkers in clinical settings can be assessed using receiver operating characteristic (ROC) curves.

2.5 | Gene set enrichment analysis (GSEA) of biomarkers related to DFU

Based on the median expression levels of biomarkers related to DFU, we categorized the samples into groups with high and low expression. Subsequently, we employed GSEA software to analyse the enrichment of the genes that were highly ranked in these two groups with regard to pathways. Herein, we used the C2.CP KEGG. v7.2 gene set sourced from the MSigDB database. The gene set permutations for each analysis were fixed at 1000. Subsequently, the gene set exhibiting significant differences was identified by applying a nominal (NOM) *p* value threshold of <0.05 and an error detection rate (FDR) q value threshold of <0.25. GeneMANIA (https://genemania.org/) can discover functionally similar genes or proteins using a large amount of genomics and proteomics data and weight each functional genomic dataset according to the predicted value of the query.[31] Therefore, we also use GeneMANIA to explore co-expressed genes for biomarkers and construct co-expressed gene networks.

2.6 | Immune infiltration analysis

To estimate the abundance of 22 different types of immune cells in tissues, the CIBERSORT deconvolution approach was used in the current study. Accordingly, the CIBERSORT method used linear support vector regression to quantify the proportion of 22 distinct immune cell types in the DFU queue. Additionally, the Wilcoxon test was used to assess differences in immune cell levels between the DFU samples and control samples.

2.7 | Quantitative reverse transcription-polymerase chain reaction (qRT-PCR)

The total RNA was extracted using TRIzol reagent (Thermo Fisher, USA). The RNA obtained from each sample (2 μg) was analysed using quantitative reverse transcription polymerase chain reaction (qRT-PCR) with FastStart Universal SYBR Green Master (Roche, Switzerland) on a LightCycler 480 PCR System (Roche, USA). The cDNA was used as a template in a reaction volume of 20 μL (2 μL of cDNA template, 10 μL of PCR mixture, 0.5 μL of forward and reverse primers and an appropriate volume of water). The PCR reactions were performed according to the following protocols: The process of initial DNA denaturation was carried out using cycling conditions, with a duration of 30 s at a temperature of 95°C. Subsequently, a total of 45 cycles were performed, each lasting 15 s at 94°C, followed by 30 s at 56°C and finally 20 s at 72°C. Three different analyses were conducted for each sample. The data obtained from the threshold cycle (CT) were collected and adjusted to the levels of GAPDH for each sample using the $2^{-\Delta\Delta CT}$ method. The mRNA expression levels were compared to those of controls obtained from healthy tissues. The primer pair sequences for the target genes are shown in Table 1.

2.8 | Western blot

For the Western blot analysis, protease and phosphatase inhibitors were added after the lumbar disc was lysed in RIPA buffer (Solarbio, China). Subsequently, the samples were denatured at 100°C for 15 min. The protein samples were transferred onto polyvinylidene fluoride (PVDF) membranes. Following a 2-h incubation period,

Gene	Forward primer sequence (5′-3′)	Reverse primer sequence (5′-3′)
HMOX1	CCAGGCAGAGAATGCTGAGTTC	AAGACTGGGCTCTCCTTGTTGC

TABLE 1 The primer pair sequences for the target genes.

PVDF membranes were blocked using a 5% solution of skimmed milk powder. The membranes were incubated overnight with an anti-HMOX1 antibody (1:500, NOVUS, NBP1-31341). Subsequently, the Chemidoc detection system (Bio-Rad, USA) was used to detect the signals from the protein strips.

2.9 | HE staining

In order to promote hydration, the portions were progressively immersed in decreasing alcohol concentrations prior to being rinsed with distilled water. After being stained with haematoxylin for 10–15 min, the sections were subsequently counterstained with 0.5% eosin for 2–5 min. In order to promote dehydration, the sections were then immersed in increasingly concentrated alcohol solutions prior to being cleansed with xylene and mounted on glass slides.

2.10 | Statistical analysis

The statistical analysis of all data was performed using R (v4.2.1). Additionally, Student's *t*-test was used to compare the two groups. Moreover, we calculated the area under the curve (AUC) of the survival receiver operating characteristic (ROC) curve to assess the clinical effectiveness of biomarkers. The significance level was set at a *p*-value of <0.05.

3 | RESULTS

3.1 | Identification of marker genes for macrophage subpopulations related to DFU

The single-cell dataset (GSE223964) was analysed at first. Following the implementation of quality control measures, we eliminated the cells that did not meet the required criteria (Figure 2A). Figure 2B displays a strong positive correlation between sequencing depth and gene number, as indicated by a coefficient of 0.89. Following the process of data normalization, we identified and selected the top 2000 genes that exhibited a high degree of variability. (Figure 2C) To reduce dimensionality, we used the PCA method, as illustrated in Figure 2D. Subsequently, by utilizing ElbowPlot and PC heat maps, we identified 14 principal components (PCs) that were most suitable for further analysis (Figure 2E,F). Based on the results of the clustering tree, we decided to use a resolution of 1.5 (Figure 2G). Figure 2H shows the heatmap representing the marker genes associated with each subgroup. Additionally, Figure 2I demonstrates that the UMAP algorithm exhibits 25 distinct cell subpopulations. By utilizing the Cellmaker database, we obtained pertinent genes and subsequently annotated 25 distinct cell subpopulations (Figure 2J). Accordingly, cell subpopulations 6 and 17 are annotated as macrophage subpopulations. Finally, we selected 802 marker genes specifically for the purpose of analysing macrophage subpopulations.

3.2 | Identification and functional annotation analysis of DEGs between normal and DFU samples

We consolidated four DFU-independent GEO datasets into a single DFU queue in this study. Subsequently, we standardized the samples from the DFU queue.(-Figure 3A,B) Then, we identified 743 DEGs and represented them using thermal and volcanic maps (Figure 3C,D). Then, an intersection analysis was performed between the DEGs and 802 marker genes specific to macrophage subpopulations. This analysis yielded 37 genes that were associated with macrophages. Additionally, the GO analysis (Figure 3E) revealed that in the BP category, these genes were primarily enriched in biological functions related to sulphur compound metabolism, regulation of anion transmembrane transport and sulphur compound biosynthesis (Figure 3F). Moreover, within the context of MF, these genes were found to be predominantly associated with specific biological functions, including the catalytic activity of alkyl or aryl groups other than methyl transfer, the binding of vascular endothelial growth factors and the binding of sulphates (Figure 3G). Furthermore, within the context of CC, these genes were primarily enriched in biological processes such as vesicle membrane, adhesion junction and lysosomal cavity (Figure 3H). The KEGG analysis demonstrates that these genes are R enriched in metabolic pathways, fluid shear stress and atherosclerosis, glutathione metabolism, fatty acid metabolism and other biological pathways (Figure 3I).

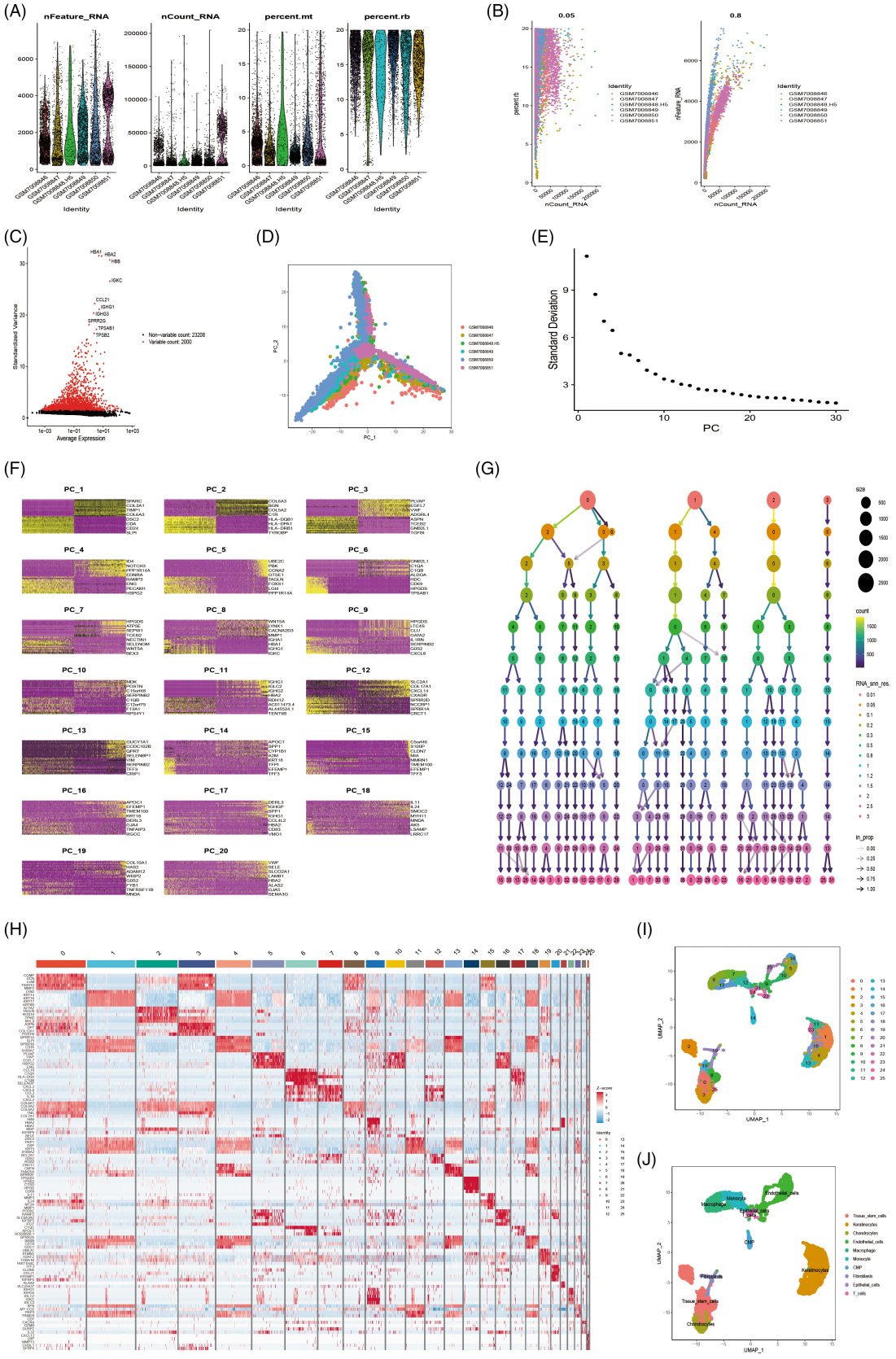

FIGURE 2 Legend on next page.

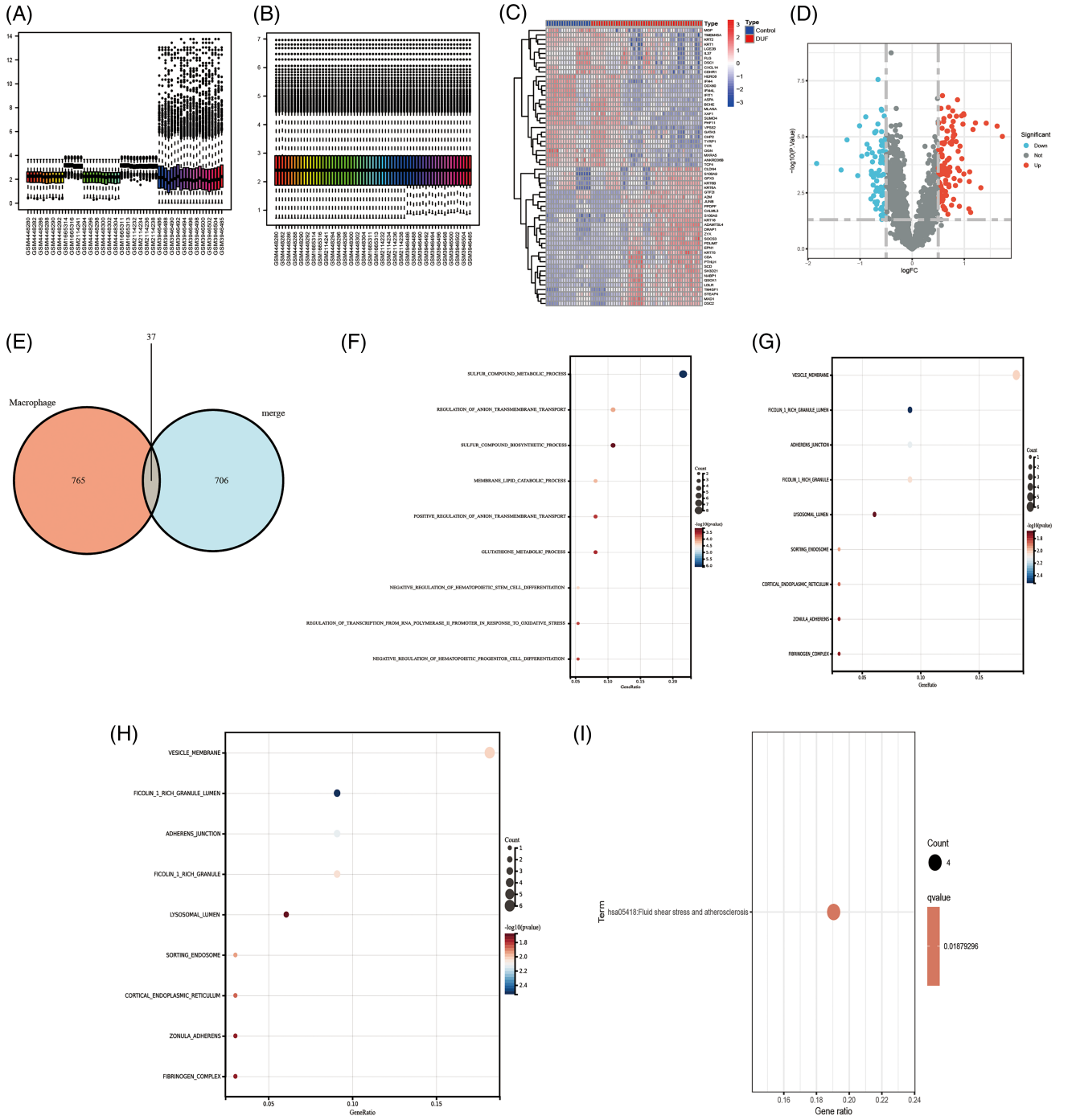

FIGURE 3 Identification of differentially expressed genes (DEGs) between normal and DFU samples. (A, B) Datasets before and after standardization. (C) Heat map of DEGs. (D) Volcano maps of DEGs. (E) The Wayne diagram shows the intersection of genes between DEGs and the marker genes of macrophage subpopulations. GO analysis of (F–H) intersection genes. (F): BP; (G): MF; (H): KEGG analysis of CC. (I) intersection genes.

FIGURE 2 Identification of marker genes for macrophage subpopulations. (A) Quality control of single-cell data. (B) Correlation analysis between sequencing depth and mitochondrial genes. (C) Red represents 2000 highly variable genes and highlights the top 10 highly variable genes. (D) Single-cell expression profiles were analysed using principal component analysis (PCA) to determine the optimal Elbowplot and heatmap for PC. (G) Select the appropriate resolution based on the clustering tree. (H) The heat map displays the expression level of marker genes for each subgroup. (I) The UMAP algorithm displays 25 cell subpopulations. (J) 25 cell subpopulations were annotated as 10 subpopulations.

3.3 | Identification of DFU-related biomarkers

The present study employed machine learning methods, viz., Boruta, XGBoost, RF and SVM-RFE, to identify potential biomarkers associated with DFU. Correspondingly, utilizing the Boruta algorithm, we successfully identified 14 distinct genes that were specifically associated with DFU from the pool of macrophage-related genes (Figure 4A,B). In addition, the use of the XGBoost algorithm successfully resulted in the identification of 20 feature genes. (Figure 4C) Furthermore, the use of the SVM-RFE algorithm, resulted in the effective screening of 37 overlapping genes and identified nine feature genes. (Figure 4D,E) Moreover, the RF algorithm successfully identified five distinct genes (Figure 4F,G). Finally, we combined the distinctive genes recognized by the four algorithms, resulting in the identification of FGL2 and HMOX1 as potential biomarkers associated with DFU (Figure 4H).

Subsequently, we analysed the expression levels of FGL2 and HMOX1 in both normal and DFU samples within the DFU queue. The expression level of FGL2 was found to be significantly higher in normal samples in comparison to the DFU samples (Figure 4I). Furthermore, the expression level of HMOX1 was significantly higher in the DFU samples, in comparison to the control samples (Figure 4J). In addition, we assessed the clinical diagnostic precision of FGL2 and HMOX1 using ROC analysis. The analysis revealed that the AUC value of FGL2 was 0.721 (Figure 4K). Thus, FGL2 exhibited significant clinical diagnostic utility. In addition, the AUC

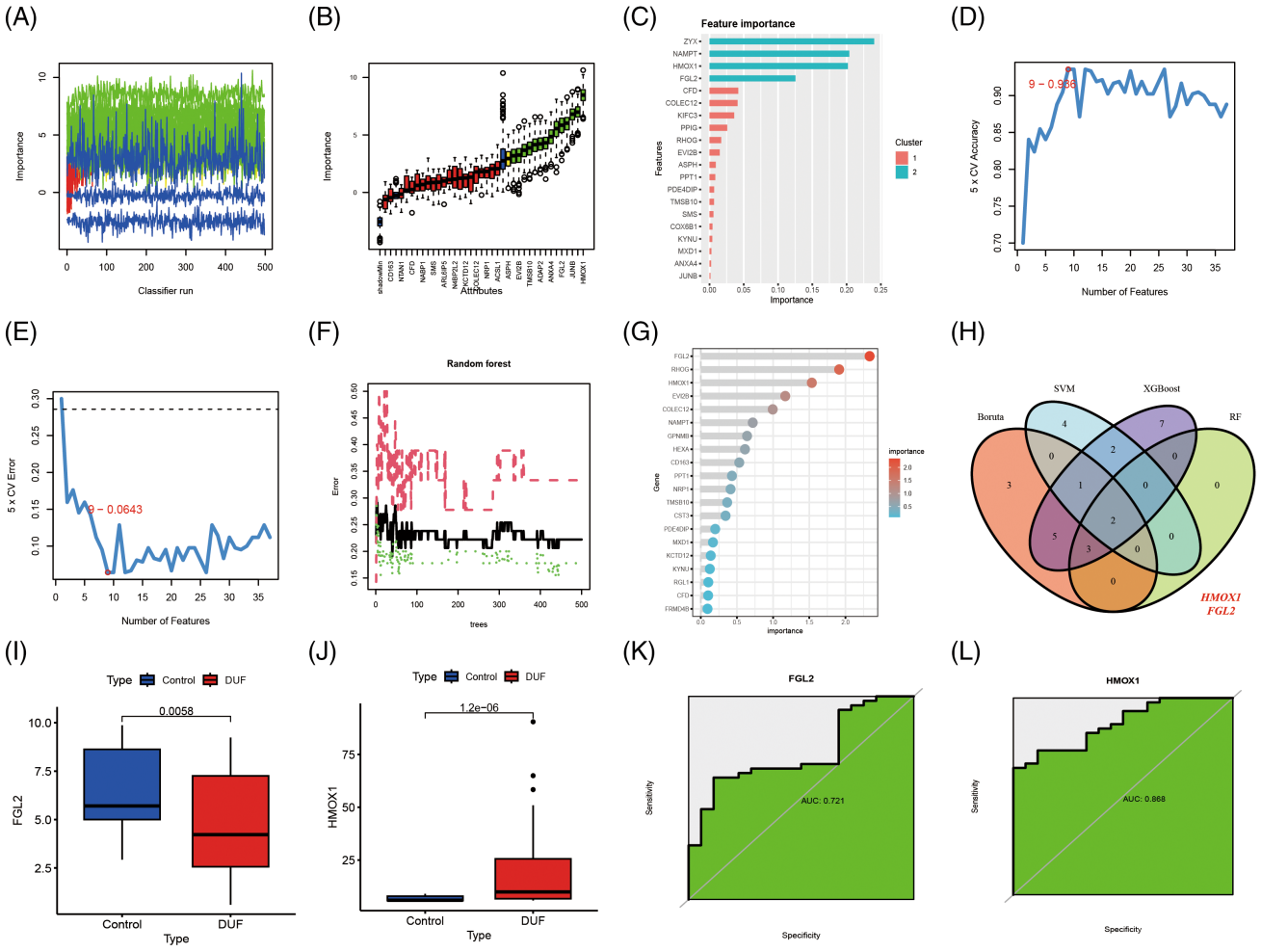

FIGURE 4 Identification of potential biomarkers for DFU. (A) The *z*-score evolution with the Boruta run (B) Selected genes by the Boruta algorithm; (C) XGBoost algorithm. (D, E) SVM-RE algorithm. (F) RF algorithm. (G) Genes ranked in the top 20 in importance. (H) The Wayne diagram shows the identification of characteristic genes related to DFU. (I) There is a significant difference in the expression of FGL2 between DFU samples and normal samples. (J) There is a significant difference in the expression of HMOX1 between DFU samples and normal samples. (K) Evaluation of clinical diagnostic accuracy of FGL2 by ROC. (L) Evaluation of clinical diagnostic accuracy of HMOX1 by ROC.

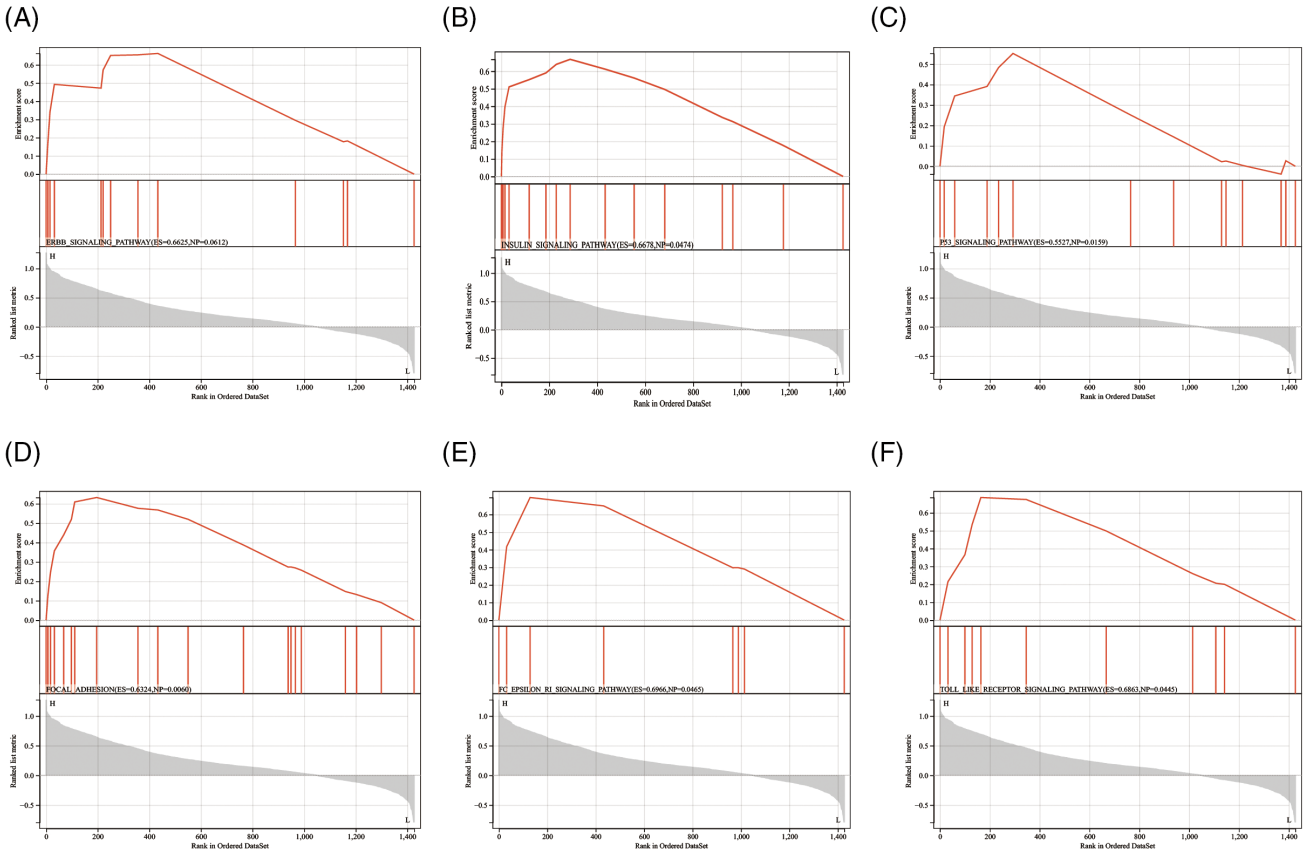

FIGURE 5 Gene set enrichment analysis analysis of HMOX1. (A) ERBB signalling pathway; (B) Insulin signalling pathway; (C) P53 signalling pathway; (D) focal adhesion; (E) FC epsilon RI signalling pathway; (F) Toll-like receptor signalling pathway.

value of HMOX1 was 0.868 (Figure 4L), which confirmed that HMOX1 had exceptional clinical diagnostic significance. Consequently, we incorporated HMOX1 in the subsequent analysis.

3.4 | GSEA analysis of HMOX1

We also conducted GSEA analysis to elucidate the role of HMOX1 in DFU and its potential mechanism of action. Correspondingly, HMOX1 was found to be involved in various biological processes, such as the ERBB, insulin, P53, focal adhesions, Fc epsilon ri and Toll-like receptor signalling pathways (Figure 5).

3.5 | Identification of HMOX1-interacting genes

We utilized GeneMANIA to create a gene–gene interaction network for HMOX1 and other related genes. The 20 genes that were associated with HMOX1 are shown in Figure 6A. As observed in Figure 6B, the functional analysis revealed a significant correlation between the fluid shear stress of these genes and important biological processes, including atherosclerosis, porphyrin metabolism and iron death. Moreover, in the GO analysis, these genes were significantly linked to multiple metabolic processes, including haeme catabolism, pigment catabolism, porphyrin-containing compound catabolism and tetrapyrrole catabolism (Table 2).

3.6 | Correlation between HMOX1 and immune cells

In addition to the above, the CIBERSORT method was employed to analyse each sample in the DFU queue and determine the estimated proportion of immune cells. When compared to normal samples, the results indicated a significant increase in the levels of naïve B cells, monocytes, resting dendritic cells and eosinophils in the DFU samples (Figure 7A). In contrast, the normal samples exhibited a substantial increase in the levels of T-cell regulation (Tregs), Plasma cells, memory B cells and macrophages M1 (Figure 7B). More importantly, HMOX1 exhibited a significant positive correlation with various immune cells, including T cells gamma delta, naïve B

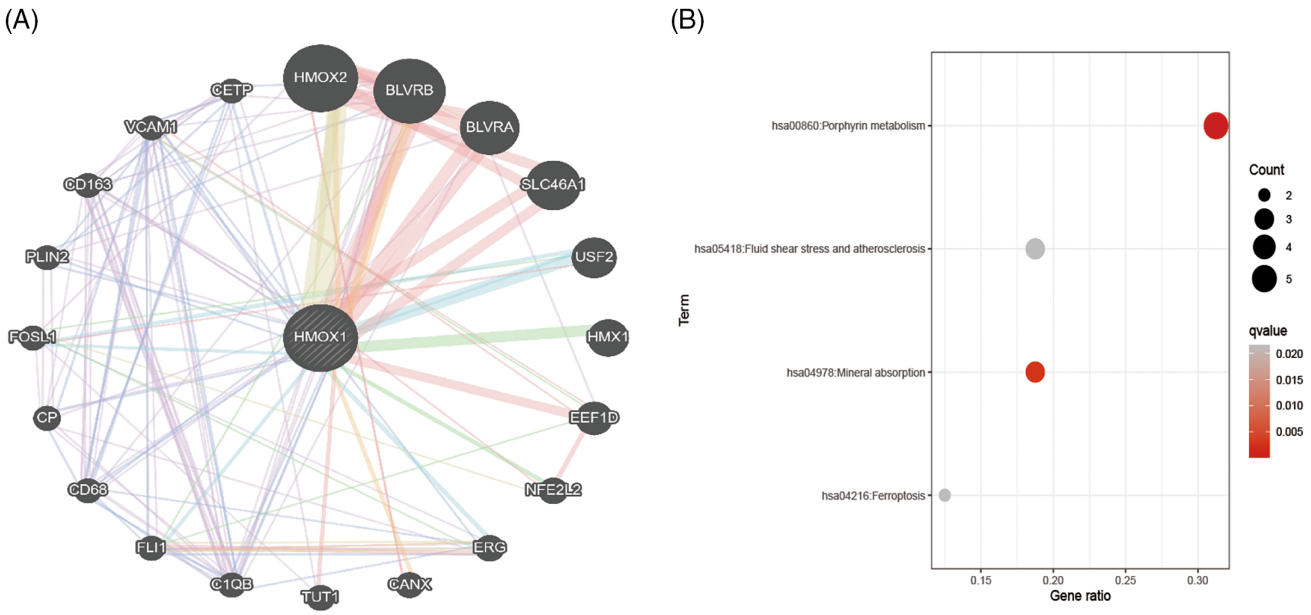

FIGURE 6 Identification of HMOX1-interacting genes. (A) 20 genes closely related to HMOX1 from GeneMania. (B) KEGG analysis.

TABLE 2 GO analysis of the 20 genes evaluated in the current study.

ONTOLOGY	ID	Description	*p* value	FDR	Count
BP	GO:0042167	Haeme catabolic process	<0.001	<0.001	4
BP	GO:0046149	Pigment catabolic process	<0.001	<0.001	4
BP	GO:0006787	Porphyrin-containing compound catabolic process	<0.001	<0.001	4
BP	GO:0033015	Tetrapyrrole catabolic process	<0.001	<0.001	4
BP	GO:0042168	Haeme metabolic process	<0.001	<0.001	5
MF	GO:0016628	Oxidoreductase activity, acting on the CH—CH group of donors, NAD or NADP as acceptor	<0.001	0.024067	2
MF	GO:0001228	DNA-binding transcription activator activity, RNA polymerase II-specific	0.001764	0.024067	4
MF	GO:0001216	DNA-binding transcription activator activity	0.00182	0.024067	4
MF	GO:0016627	Oxidoreductase activity, acting on the CH—CH group of donors	0.002117	0.024067	2

cells, activated NK cells, eosinophils, monocytes and others. HMOX1 exhibits a strong negative correlation with immune cells including macrophages M1, plasma cells, macrophages M2 and others (Figure 7C).

3.7 | Experimental verification of the clinical value of HMOX1

In order to assess the reliability of the bioinformatics results, we conducted a qRT-PCR analysis using both normal skin tissues and ulcerated skin tissues obtained from diabetic patients. The results of qRT-PCR were consistent with those predicted using the bioinformatics approach used in the study. Accordingly, the expression of HMOX1 was found to be increased in the ulcerated skin tissues of diabetic patients (Figure 8A). This was consistent with the results of the Western blot analysis, which also indicated an increased expression of HMOX1 in DFU tissues (Figure 8B,C). Furthermore, the results of HE analysis also indicated a substantial increase in the number of immune cells in the DFU tissues (Figure 8D,E).

4 | DISCUSSION

DFU comprises a serious complication, which frequently occurs in individuals with diabetes. It is typically attributed to the nerve and vascular impairment resulting from

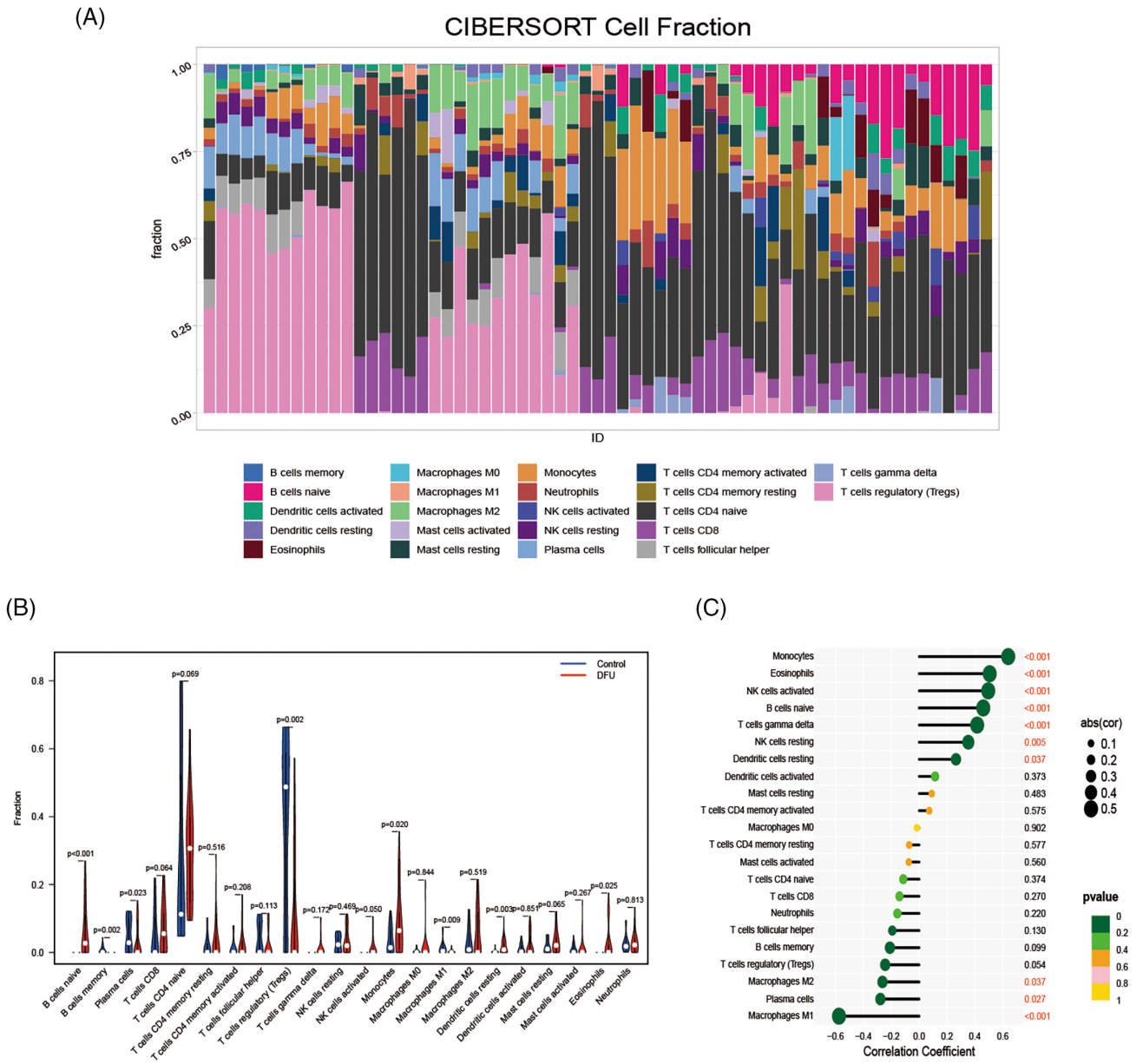

FIGURE 7 The difference in immune cell infiltration levels between normal and DFU samples. (A) The proportion of immune cells in each sample in the DFU queue. (B) Violin diagram of differential expression of immune cells in DFU samples and normal samples. (C) The correlation between HMOX1 and immune cells.

long-term hyperglycaemia, which typically manifests as chronic foot ulcers, infections and inflammation.[32] The lifetime prevalence of foot ulcer in individuals with diabetes ranges from 19% to 34%. However, the 1-year incidence rate of ulcer recurrence is estimated to be 40%, while the recurrence rate within 5 years is 65%.[7] Correspondingly, the presence of DFU has significantly impacted the well-being and financial aspects of individuals suffering from diabetes. Hence, there is an urgent need to identify precise therapeutic targets to enhance the prognosis of patients with DFU. Macrophages comprise an important subset of immune cells within the immune system and participate in inflammatory responses, wound healing and tissue regeneration processes. Dysfunction of macrophages in DFU can cause chronic inflammatory reactions, which impede the process of wound healing.[15,18,33] Hence, the present study utilized single-cell transcriptome analysis to identify specific macrophage subpopulations that are associated with DFU. By analysing the characteristic genes of these specific macrophage subpopulations, we were able to gain insights into their functions and contributions to the development of DFU. Simultaneously, this study also integrated machine learning to explore macrophage-

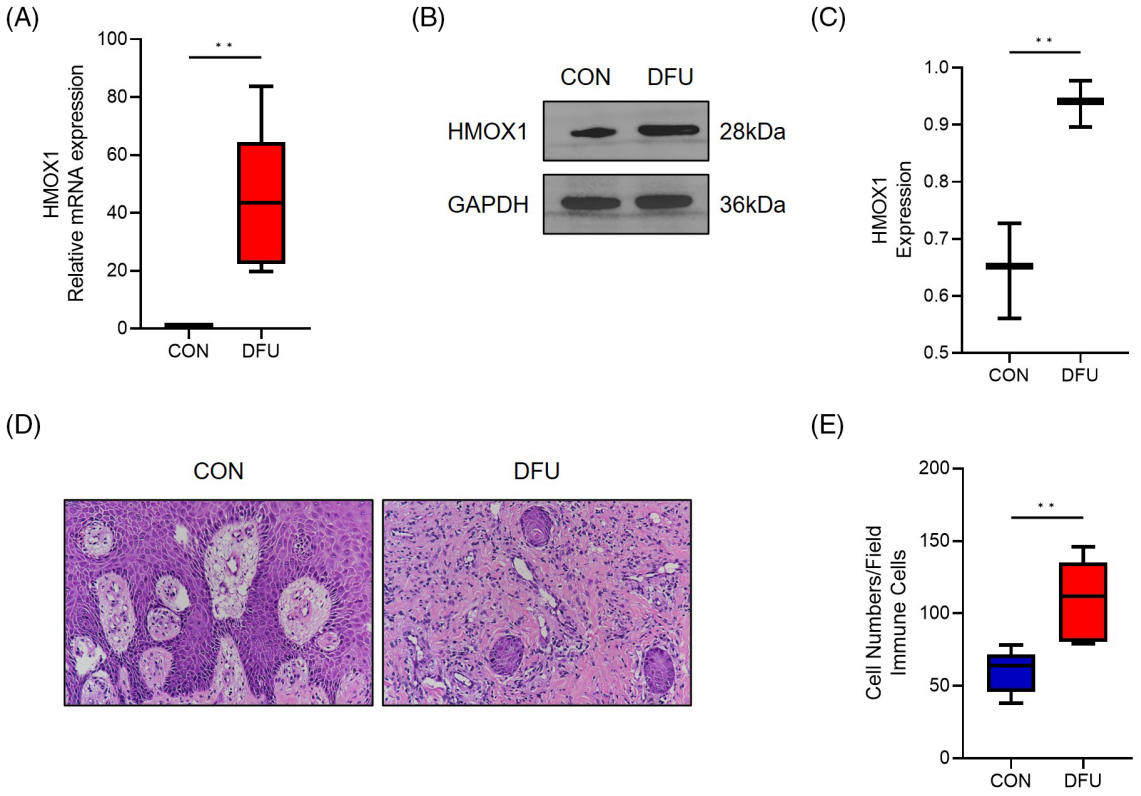

FIGURE 8 HMOX1 expression is elevated in ulcerated skin tissues of diabetic patients. (A) The mRNA expression of HMOX1 in normal skin tissues and diabetic ulcerated skin tissues was examined by qRT-PCR and analysed for relative quantification: $N = 6$. (B, C). Protein expression of DUSP1 and HMOX1 in normal skin tissues and diabetic ulcerated skin tissues was detected and quantified by WB: $N = 3$. (D, E) The number of immune cells infiltrated in normal skin tissues and diabetic ulcerated skin tissues was detected and quantified by HE: $N = 5$.

associated genes that exhibited abnormal expression in DFU, and discovered potential biomarkers associated with DFU. Thus, the present study enhances our understanding of the role of macrophages in DFU and aids in the creation of effective treatment plans for this condition.

Through the examination of single-cell data, marker genes for a total of 802 distinct subpopulations of macrophages were identified in the current study. Subsequently, the marker genes were crossed with the DEGs between normal and DFU samples, to identify 37 genes associated with macrophages. Subsequently, the GO analysis revealed that these genes were involved in specific biological processes, molecular functions and cellular components including sulfur-containing compound metabolism processes, adhesive binding and vascular endothelial growth factor binding. In addition, the KEGG analysis revealed a significant association of these genes with metabolic pathways, fluid shear stress, atherosclerosis, iron death and other biological pathways. Iron death is a cellular process of programmed cell death characterized by disrupted iron balance and excessive lipid peroxidation.[34] A high concentration of serum iron has been associated with an increased risk of developing type 2 diabetes.[35] Currently, ongoing research is being conducted to investigate the mechanism of iron death in DFU. However, a correlation does indeed exist. In this context, He et al., found that inhibitors associated with iron-induced cell death have a protective effect in DFU.[36] This suggests a strong correlation between iron death and DFU. In addition, prolonged hyperglycaemic environments can result in impairment of the iron metabolism pathway, causing a significant reduction in the number of iron binding sites in circulating transferrin and ferritin, as well as an increase in the amount of free iron in the plasma, ultimately leading to oxidative stress.[37–39] Moreover, oxidative stress is has been frequently identified as the main cause of complications associated with diabetes, such as delayed ulcer healing.[37] Consequently, an excessive buildup of iron and increased oxidative stress may result in cellular death and increased inflammatory reaction in the foot tissue, further damaging the nerves and blood vessels in the foot and impeding the healing of wounds. Thus, iron-induced cell death may contribute to the development of DFU through the aforementioned pathways. However, it is important to acknowledge that

additional investigation is required to fully understand the precise mechanism by which iron contributes to the development of complications associated with DFU.

Herein, we conducted additional screening and successfully identified potential biomarkers of DFU by utilizing four machine-learning algorithms. Accordingly, HMOX1 was identified as a promising biomarker. HMOX1 is a catalytic protein that is necessary for the breakdown of haeme. When compared with normal samples, HMOX1 showed higher expression in DFU samples. Consequently, the ROC analysis demonstrated that HMOX1 (HO-1) exhibited excellent diagnostic efficacy for DFU. The experiment also confirmed the substantial expression of HMOX1 in DFU samples. More importantly, HMOX1 exhibited a strong positive correlation with immune cells, including eosinophils, monocytes and activated NK cells. Conversely, the expression of HMOX1 showed a significant negative correlation with macrophage M1 and macrophage M2. Additionally, NRF2 is a member of the Cap-n Collar family of alkaline leucine zipper proteins and is involved in the regulation of oxidative stress and aging effects.[40] HO-1 comprises one of the downstream genes regulated by NRF2. During the process of cell aging, the NRF2/HO-1 pathway exerts a protective effect.[41] Wang et al., found that miR-181b-5p can promote cellular aging and impede the formation of new blood vessels by influencing the NRF2/HO-1 pathway. This, subsequently, hinders the process of wound healing in DFU wounds.[42] More importantly, Meng et al., discovered that the elimination of HMOX1 can diminish Fe^{2+} overload, consequently decreasing iron levels, reactive oxygen species and lipid peroxidation.[42] This further reduces the iron death of endothelial cells in patients with diabetes.[43] In order to elucidate the mechanism by which HMOX1 acts in DFU, a GSEA analysis was performed in the current study, which revealed the relationship between HMOX1 and several biological pathways, such as ERBB, insulin, P53 and toll-like receptor signalling pathways. In addition, insulin signalling plays a crucial role in the process of wound healing.[44] Insulin signalling can activate the differentiation of effector T cells into the helper T2 phenotype and decrease the ratio of interferon levels-γ/IL-4, thus facilitating anti-inflammatory activity.[45] Earlier studies show that the topical insulin on the skin surface in a rat burn wound model effectively reduces the production of ROS and minimized oxidative harm to DNA, lipids and proteins within the wound.[46] Furthermore, the application of topical insulin can facilitate the early recruitment of neutrophils to the surface of the wound, aiding in the removal of necrotic tissue in burn injuries.[46] Moreover, in diabetes rat models, local insulin treatment can improve the wound healing of diabetes rats and normalize corneal re-epithelization.[47–49] This indicates that insulin signal transduction resident in skin cells is crucial for wounds in diabetes animals. In addition, local insulin can improve the deposition of fibrillar collagen, re-epithelization, granulation and wound contraction in burn wounds of diabetes rats.[50] As observed, the insulin signalling pathway plays a crucial role in the process of wound healing in individuals with diabetes. Nevertheless, there is currently limited research on the mechanism of insulin signalling pathways in DFU. Thus, additional investigations are imperative to further explore the mechanism of insulin signalling pathways in DFU.

Nevertheless, the research is constrained in several aspects. First, the small sample size included in the study may affect the accuracy of the results, resulting in incorrect identification and missed diagnosis. Hence, the use of a larger DFU sample size to validate the accuracy of the results is imperative. Second, the HMOX1 gene discovered in this study has the potential to be a target for therapeutic interventions in DFU. However, it is necessary to validate this finding through experimental studies involving a larger number of participants.

5 | CONCLUSION

To conclude, our analysis provides critical insight into the precise action mechanisms of macrophages in DFU, elucidating their specific functions. More importantly, HMOX1 was identified as a valuable biomarker for DFU. These findings enhance our understanding of the pathophysiology of DFU and have the potential to assist in the development of more targeted approaches for managing this condition.

FUNDING INFORMATION

This work was supported by The Nantong Municipal Health Commission General Project Fund (MB2021006).

CONFLICT OF INTEREST STATEMENT

The authors declare that they have no competing interests.

DATA AVAILABILITY STATEMENT

The raw data supporting the conclusions of this manuscript will be made available by the corresponding authors, without undue reservation, to any qualified researcher.

ETHICS STATEMENT

The experimental protocol was established, according to the ethical guidelines of the Helsinki Declaration and was approved by the Ethics Committee of Nantong University Affiliated Hospital (2022-K034-02).

CONSENT TO PARTICIPATE

Each participant provided the written informed consent for participation.

REFERENCES

1. Chen XW, Ding G, Xu L, Li P. A glimpse at the metabolic research in China. *Cell Metab*. 2021;33(11):2122-2125.
2. Artasensi A, Pedretti A, Vistoli G, Fumagalli L. Type 2 Diabetes Mellitus: A Review of Multi-Target Drugs. *Molecules*. 2020; 25(8):1987.
3. Jaiswal V, Negi A, Pal T. A review on current advances in machine learning based diabetes prediction. *Prim Care Diabetes*. 2021;15(3):435-443.
4. Chatwin KE, Abbott CA, Boulton AJM, Bowling FL, Reeves ND. The role of foot pressure measurement in the prediction and prevention of diabetic foot ulceration-a comprehensive review. *Diabetes Metab Res Rev*. 2020;36(4):e3258.
5. Liu Y, Liu Y, Deng J, Li W, Nie X. Fibroblast growth factor in diabetic foot ulcer: Progress and therapeutic prospects. *Front Endocrinol*. 2021;12:744868.
6. Barrett T, Wilhite SE, Ledoux P, et al. NCBI GEO: Archive for functional genomics data sets—update. *Nucleic Acids Res*. 2013; 41:D991-D995.
7. Armstrong DG, Boulton AJM, Bus SA. Diabetic foot ulcers and their recurrence. *N Engl J Med*. 2017;376(24):2367-2375.
8. Hoffstad O, Mitra N, Walsh J, Margolis DJ. Diabetes, lower-extremity amputation, and death. *Diabetes Care*. 2015;38(10): 1852-1857.
9. Meloni M, Izzo V, Giurato L, Lázaro-Martínez JL, Uccioli L. Prevalence, clinical aspects and outcomes in a large cohort of persons with diabetic foot disease: Comparison between neuropathic and ischemic ulcers. *J Clin Med*. 2020;9(6):1780.
10. Deng Z, Ou H, Ren F, et al. LncRNA SNHG14 promotes OGD/-R-induced neuron injury by inducing excessive mitophagy via miR-182-5p/BINP3 axis in HT22 mouse hippocampal neuronal cells. *Biol Res*. 2020;53(1):38.
11. Bardill JR, Laughter MR, Stager M, Liechty KW, Krebs MD, Zgheib C. Topical gel-based biomaterials for the treatment of diabetic foot ulcers. *Acta Biomater*. 2022;138:73-91.
12. Baltzis D, Eleftheriadou I, Veves A. Pathogenesis and treatment of impaired wound healing in diabetes mellitus: new insights. *Adv Ther*. 2014;31(8):817-836.
13. Spiller KL, Koh TJ. Macrophage-based therapeutic strategies in regenerative medicine. *Adv Drug Deliv Rev*. 2017;122:74-83.
14. Kotwal GJ, Chien S. Macrophage differentiation in Normal and accelerated wound healing. *Results Probl Cell Differ*. 2017;62:353-364.
15. Lin CW, Hung CM, Chen WJ, et al. New horizons of macrophage immunomodulation in the healing of diabetic foot ulcers. *Pharmaceutics*. 2022;14(10):2065.
16. Louiselle AE, Niemiec SM, Zgheib C, Liechty KW. Macrophage polarization and diabetic wound healing. *Transl Res: J lab Clin Med*. 2021;236:109-116.
17. Krzyszczyk P, Schloss R, Palmer A, Berthiaume F. The role of macrophages in acute and chronic wound healing and interventions to promote pro-wound healing phenotypes. *Front Physiol*. 2018;9:419.
18. Aitcheson SM, Frentiu FD, Hurn SE, Edwards K, Murray RZ. Skin wound healing: Normal Macrophage Function and Macrophage Dysfunction in Diabetic Wounds. *Molecules*. 2021; 26(16):4917.
19. Lin CW, Chen CC, Huang WY, et al. Restoring Prohealing/remodeling-associated M2a/c macrophages using ON101 accelerates diabetic wound healing. *JID Innovation: Skin Science from Molecules to Population Health*. 2022;2(5):100138.
20. Hu J, Wang L, Li L, Wang Y, Bi J. A novel focal adhesion-related risk model predicts prognosis of bladder cancer—a bioinformatic study based on TCGA and GEO database. *BMC Cancer*. 2022;22(1):1158.
21. Chen Y, Huang W, Ouyang J, Wang J, Xie Z. Identification of Anoikis-related subgroups and prognosis model in liver hepatocellular carcinoma. *Int J Mol Sci*. 2023;24(3):2862.
22. Xia WT, Qiu WR, Yu WK, Xu ZC, Zhang SH. Identifying TME signatures for cervical cancer prognosis based on GEO and TCGA databases. *Heliyon*. 2023;9(4):e15096.
23. Yang Y, Cao Y, Han X, et al. Revealing EXPH5 as a potential diagnostic gene biomarker of the late stage of COPD based on machine learning analysis. *Comput Biol Med*. 2023;154:106621.
24. Kolodziejczyk AA, Kim JK, Svensson V, Marioni JC, Teichmann SA. The technology and biology of single-cell RNA sequencing. *Mol Cell*. 2015;58(4):610-620.
25. Armand EJ, Li J, Xie F, Luo C, Mukamel EA. Single-cell sequencing of brain cell transcriptomes and Epigenomes. *Neuron*. 2021;109(1):11-26.
26. Chambers DC, Carew AM, Lukowski SW, Powell JE. Transcriptomics and single-cell RNA-sequencing. *Respirology (Carlton, Vic)*. 2019;24(1):29-36.
27. Ogunleye A, Wang QG. XGBoost model for chronic kidney disease diagnosis. *IEEE/ACM Trans Comput Biol Bioinform*. 2020; 17(6):2131-2140.
28. Garge NR, Bobashev G, Eggleston B. Random forest methodology for model-based recursive partitioning: the mobForest package for R. *BMC Bioinformatics*. 2013;14:125.
29. Sanz H, Valim C, Vegas E, Oller JM, Reverter F. SVM-RFE: selection and visualization of the most relevant features through non-linear kernels. *BMC Bioinformatics*. 2018;19(1):432.
30. Kursa MB. Robustness of random Forest-based gene selection methods. *BMC Bioinformatics*. 2014;15:8.
31. Warde-Farley D, Donaldson SL, Comes O, et al. The GeneMANIA prediction server: biological network integration for gene prioritization and predicting gene function. *Nucleic Acids Res*. 2010;38:W214-W220.
32. Singh N, Armstrong DG, Lipsky BA. Preventing foot ulcers in patients with diabetes. *JAMA*. 2005;293(2):217-228.
33. Mirza RE, Fang MM, Ennis WJ, Koh TJ. Blocking interleukin-1β induces a healing-associated wound macrophage phenotype and improves healing in type 2 diabetes. *Diabetes*. 2013;62(7): 2579-2587.
34. Dixon SJ, Lemberg KM, Lamprecht MR, et al. Ferroptosis: an iron-dependent form of nonapoptotic cell death. *Cell*. 2012; 149(5):1060-1072.
35. Sha W, Hu F, Xi Y, Chu Y, Bu S. Mechanism of Ferroptosis and its role in type 2 diabetes mellitus. *J Diabetes Res*. 2021; 2021:9999612.
36. He J, Li Z, Xia P, et al. Ferroptosis and ferritinophagy in diabetes complications. *Mol Metab*. 2022;60:101470.
37. Feng J, Wang J, Wang Y, et al. Oxidative stress and lipid peroxidation: prospective associations between Ferroptosis and

delayed wound healing in diabetic ulcers. *Front Cell Dev Biol*. 2022;10:898657.
38. Alavi A, Sibbald RG, Mayer D, et al. Diabetic foot ulcers: part I. Pathophysiology and prevention. *J Am Acad Dermatol*. 2014;70(1):e1-e18. quiz 19-20.
39. Jiang QW, Kaili D, Freeman J, et al. Diabetes inhibits corneal epithelial cell migration and tight junction formation in mice and human via increasing ROS and impairing Akt signaling. *Acta Pharmacol Sin*. 2019;40(9):1205-1211.
40. Loboda A, Damulewicz M, Pyza E, Jozkowicz A, Dulak J. Role of Nrf2/HO-1 system in development, oxidative stress response and diseases: An evolutionarily conserved mechanism. *CMLS*. 2016;73(17):3221-3247.
41. Romero A, San Hipólito-Luengo Á, Villalobos LA, et al. The angiotensin-(1-7)/mas receptor axis protects from endothelial cell senescence via klotho and Nrf2 activation. *Aging Cell*. 2019;18(3):e12913.
42. Wang S, Shi M, Zhou J, Wang W, Zhang Y, Li Y. Circulating Exosomal miR-181b-5p promoted cell senescence and inhibited angiogenesis to impair diabetic foot ulcer via the nuclear factor erythroid 2-related factor 2/Heme Oxygenase-1 pathway. *Front Cardiovasc Med*. 2022;9:844047.
43. Meng Z, Liang H, Zhao J, et al. HMOX1 upregulation promotes ferroptosis in diabetic atherosclerosis. *Life Sci*. 2021;284:119935.
44. Emanuelli T, Burgeiro A, Carvalho E. Effects of insulin on the skin: possible healing benefits for diabetic foot ulcers. *Arch Dermatol Res*. 2016;308(10):677-694.
45. Viardot A, Grey ST, Mackay F, Chisholm D. Potential antiinflammatory role of insulin via the preferential polarization of effector T cells toward a T helper 2 phenotype. *Endocrinology*. 2007;148(1):346-353.
46. Dhall S, Silva JP, Liu Y, et al. Release of insulin from PLGA-alginate dressing stimulates regenerative healing of burn wounds in rats. *Clin Sci*. 2015;129(12):1115-1129.
47. Greenway SE, Filler LE, Greenway FL. Topical insulin in wound healing: a randomised, double-blind, placebo-controlled trial. *J Wound Care*. 1999;8(10):526-528.
48. Lima MH, Caricilli AM, de Abreu LL, et al. Topical insulin accelerates wound healing in diabetes by enhancing the AKT and ERK pathways: a double-blind placebo-controlled clinical trial. *PloS One*. 2012;7(5):e36974.
49. Zagon IS, Klocek MS, Sassani JW, McLaughlin PJ. Use of topical insulin to normalize corneal epithelial healing in diabetes mellitus. *Arch Ophthalmol*. (Chicago, Ill: 1960). 2007;125(8):1082-1088.
50. Azevedo F, Pessoa A, Moreira G, et al. Effect of topical insulin on second-degree burns in diabetic rats. *Biol Res Nurs*. 2016;18(2):181-192.

How to cite this article: Chen Y, Zhang Y, Jiang M, Ma H, Cai Y. HMOX1 as a therapeutic target associated with diabetic foot ulcers based on single-cell analysis and machine learning. *Int Wound J*. 2024;21(3):e14815. doi:10.1111/iwj.14815